The Effect of Filler Loading Ratios and Moisture on DC Conductivity and Space Charge Behaviour of SiO_2 and hBN Filled Epoxy Nanocomposites

Dayuan Qiang[1,2], Yan Wang[1,2], Xinyu Wang[1,2], George Chen[1,2] and Thomas Andritsch[1,2]

[1] School of Electronic and Computer Science, University of Southampton, Southampton, United Kingdom
[2] The Tony Davis High Voltage Laboratory, University of Southampton, Southampton, United Kingdom

E-mail: opstraxex@gmail.com

Received xxxxxx
Accepted for publication xxxxxx
Published xxxxxx

Abstract

Nanocomposites those exhibit good insulation properties have already attracted numbers of research and their electrical properties are believed to be related to charge dynamics in bulk of materials. However, it is still unclear on how nanofiller loading ratios, surface treatment and resultant changes in morphology influence the charge dynamics of nanocomposites. In this paper, we have clearly mentioned the influence of adding nanoparticles into epoxy resins and the characteristics of the movement of charges in the materials based on combining analysis on morphology, DC conductivity and space charge measurements. The presence of spherical nanoparticles (SiO_2) introduced additional traps in bulk, which impaired the charge injection and reduced the mobility of charge carriers in samples of low filler loading ratios (e.g., 0.5 wt%). However, in silica-based samples of higher filler loadings, more nanoparticles further caused a higher density of traps, which resulted in lower average distance between arbitrary traps/ inter-particle surface distances and thus charge carriers required less energy when moving from one to another by hopping or the quantum tunnelling mechanism. The surface treatment of SiO_2 particles introduced deep traps which helped the separation of particles or related traps, and to some extent restricted the transport of charge carriers. In addition, hBN particles seem to act as barriers to charge injection and movement due to the layered structures and large numbers of resultant shallow traps in bulk. In term of moisture effect, the presence of water led to an obvious increase in charge injection and mobility, and resulted in the higher mobility of charge carriers in both base materials and within traps/particles of nanocomposites. The existence of water shells around spherical particles could contribute to a higher probability of the quantum tunnelling process and the formation of conductive percolation channels.

Keywords: epoxy nanocomposites, electrical properties, charge dynamics, hopping and tunnelling process, moisture

1. Introduction

Epoxy resins are types of epoxy oligomers, which generally refer to organic molecules without high molecular mass, have excellent adhesion, chemical and heat resistance, mechanical properties, and insulating properties. It is one of the most commonly used thermosetting materials in high voltage apparatus as insulation, owing to its good mechanical and electrical properties, and chemical stability [1]. Because nanoparticles are potentially to reinforce properties of unfilled epoxy, its nanocomposites have attracted broad interest [2-4]. Owing to the unique characteristics of nano-size fillers, nanoparticle reinforced epoxy resins displayed obvious improvements in their properties [5, 6], however, introducing nanofillers can also sometimes result in a reduction of insulation properties or insignificant changes [7, 8].

When a sufficiently high electric field is applied to epoxy resins, charges can be injected into the bulk of materials, and could travel within the material under an external electric field. In this case, the electrical properties of the epoxy resin would also be changed. This change is not only due to the high applied field, but also the temperature, the electrode and polymer interface [9]. Earlier studies have also found that charge trapping, tunnelling and hopping conduction determine the charge transport in the materials [10-13]. There are few kinds of literature which report electrical conduction of silica and boron nitride based nanocomposites [14-17]. Most of their results show an increase in direct current (DC) conductivity when the fillers are introduced, while results from *Hui* et al. indicate conductivity only increased in the samples of high filler loading ratios with moisture [14].

In term of space charge, it is a surplus of charge carriers, including electrons, ions and holes distributed into the polymer material. These charges are moving around and trapped in the material. The trapped charges could lead to space charge limited current (SCLC), which causes electrical breakdown or aging problems of the polymer when the applied electric field is high enough [10]. Space charge usually occurs in dielectric material and is one of the most important factors that will decide the dielectric properties of the material [12]. The space charges mainly come from the electrode injection and generation within the polymer materials [18]. Earlier studies have also shown that the presence of nanofillers in the epoxy resin influences the accumulation of space charge. When compared to pure epoxy, epoxy nanocomposites seem to have less accumulated charges. It has also been reported that the dynamics of charges in epoxy nanocomposites result in faster-charging intensity, especially for negative charges. Results by *Fabiani* et al. indicate the space charge built-up and charge mobility are obviously influenced by filler loadings [19]. Moreover, Some researchers believe that the improvements in properties of epoxy resins result from the surface effects of nanoparticles [20, 21]. *Andritsch* et al. point out changes in the structure due to the introduction of nanoparticles and surface functionalisation could contribute to the unique space charge behaviour of epoxy nanocomposites. They also remarked the different results due to introducing different nanofillers [19]. Thus, the type of filler is also an important factor affecting the properties, and they must be chosen carefully.

In addition, epoxy has the problem of absorbing water from humid ambient environments, and the loaded fillers could exacerbate or even lead to the formation of water shells, as studied by *Zou* et al. This is the result of free volume and hydroxyl groups on the surface of nanoparticles [22]. Further, *Hui* et al. hypothesised the formation of water shell surrounding the particles and consequent changes in the inter-particle/aggregate distances are two major factors affecting the dielectric behavior and percolation of silica-based nanocomposites [14]. *Hosier* et al. studied the effects of water on the dielectric properties of PE nanocomposites, and based on this they simulated the water shell and resulting percolation. They concluded the dramatic effects of moisture compared to the dispersion of particles, and emphasised the importance of understanding and controlling environmental water during industrial practices [23]. However, there are few studies focusing on epoxy based nanocomposites.

Therefore, in this paper, we employ a range of epoxy nanocomposites to investigate specific objectives as below:

(i) To investigate the effect of filler loading ratios and moisture on charge dynamics of epoxy nanocomposites.

(ii) To investigate the effect of nanofillers, surface treatment and resultant changes in morphology on charge dynamics: nanoparticles introduced in this work are nano silica (with and without surface treatment) and hexagonal boron nitride (hBN).

2. Experiment Preparation

2.1 Materials

The samples for testing were prepared based on bisphenol-A diglycidyl ether (D.E.R. 332, density 1.16 $g \cdot cm^{-3}$) cured with polyether amine hardener (Jeffamine D-230, density 0.948 $g \cdot cm^{-3}$) supplied by Huntsman. The nanoparticles used in the study are commercially available untreated SiO_2 and hexagonal boron nitride (hBN) provided by Sigma-Aldrich and Momentive respectively. More information is detailed and listed in Table 1. Moreover, trimethoxy (octyl) silane was used as coupling agent to produce C8-treated nano SiO_2 in order to remove the hydroxyl groups on surface of SiO_2 particles and form relatively hydrophobic and unfunctional surface structures for better dispersion of particles. In addition, film samples were prepared with a thickness of 0.145 ± 0.01 mm. In the process of sample preparation, epoxy and its nanocomposites were cured at 120 ℃ for 4 hours with the ratio between epoxy resin and hardener was 1000:344 [24].

Filler loading ratios of nanoparticles are 0.5, 1, 3 and 5 wt%, and following abbreviations are used while coding the samples: EP for epoxy resin, **S** for untreated nano silica composites, **ST** for treated silica, **B** for boron nitride and the number represents the filler loading. For example, EPS05 represents epoxy nanocomposites filled with 0.5 wt% untreated silica and EPST1 is for 1 wt% treated silica loaded epoxy nanocomposites.

Table 1 Particle information

Type	Size (*nm*)	Shape
SiO_2	10-20 (BET)	Spherical
hBN	900 (APS) 200-500 (Crystal Size)	Hexagonal Platelets

2.2 Sample Conditioning

There are four relative humidity (RH) conditions in the test.

- All dry samples were held in the vacuum oven (103 Pa, 60 ºC, for 72 h) and then stored in a vacuum desiccator with dried silica gel at 293 K.
- Ambient Humidity (A.RH): These samples were exposed to the laboratory environment for 10 days where temperature and RH were controlled at 293 K and (36.1 ± 6.7) %.
- 60% RH: These samples were stored in a RH controlled chamber at 293 K, where actual RH is in the range from 56 to 62%.
- Saturated: These samples were immersed in de-ionised water for 10 days before testing at 293 K.

The samples were held in a humid environment but were periodically removed and weighed using a microbalance. The measurements were continued until the weight becomes stable. This took about 10 days in A.RH, 60% RH and totally saturated environments.

2.3 Characterisation Methods

EVO 50 scanning electron microscopy (SEM) was used to characterise the morphology of epoxy and its nanocomposites. The gun voltage was set to 15 kV with a working distance of 7-12 mm. All samples were coated with gold before the test by the Emitech K550X sputter coater at 25 mA for 3 min for each sample.

DC conductivity measurements were carried out on samples that were pre-conditioned in different humidity environments. Before DC conductivity testing the thin film samples were sputter coated with gold to create electrodes on both sides with a diameter of 30 mm. The sample was then placed between two parallel electrodes (20 mm in diameter) and a voltage between 5 and 6 kV was applied in order to achieve an average electric field of ~40 kV·mm^{-1} inside the sample. A Keithley 6487 pico-ammeter was used to measure the current through the specimen as a function of time, DC conductivity was then calculated from this data by software running on the experiment control computer. All the tests were carried out at 20 ºC under ambient RH conditions.

Pulsed electro-acoustic (PEA) technique was used to measure the space charge distribution in the samples [25]. The principle of the PEA measurement is to apply a short pulse voltage across the sample and then to record the acoustic vibrations that are caused by the motions of space charge that is distributed within the sample. This is shown diagrammatically in Fig. 1.

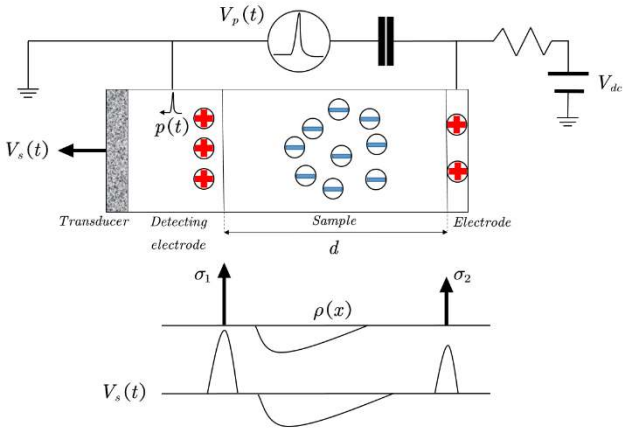

FIG. 1 Illustration of PEA method.

"Volts-on" measurements were taken in the experiments, meaning that the readings will be taken by applying a pulse when a voltage is applied to the samples. Before the measurements, a reference measurement also needs to be taken. For the epoxy resin samples, the voltage for reference measurement is set to 1.5 kV. The applied voltage during the volts-on measurements is ~5 to 6 kV. Thus, the applied electric field is maintained at 40 kV·mm^{-1}. The readings are taken using a software package called "Easy Data" at 0 seconds, 120 seconds, 300 seconds, 600 seconds, 1200 seconds, 1800 seconds, 2400 seconds, 3000 seconds and 3600 seconds. After this measurement is complete, a test of space charge decay is also processed: data is collected at 0 seconds, 30 seconds, 60 seconds, 90 seconds, 120 seconds, 150 seconds, and 180 seconds. In the interests of clarity, only selected data are presented in the results.

3. Experiment Results and Analysis

3.1 Scanning Electron Microscope

The SEM images of EPS and EPST samples are shown in Fig. 2 and 3. It is noticed that the number of particles in EPS samples increases with filler loading ratios. In 3 wt% of EPS samples, obvious agglomerations of particles/aggregates have appeared (as circled) and it seems that the fillers have had a significant impact on the structure of the matrix, especially in EPS samples shown in Fig. 2. The more perturbed matrix morphology may lead to deteriorated electrical properties in epoxy nanocomposites. Comparing EPS and EPST samples, it is easy to note that the surface treatment acts to reduce disturbance of the polymer matrix, this is especially clear for high filler ratios of SiO_2 samples when compared Fig. 2(b) with Fig. 3.

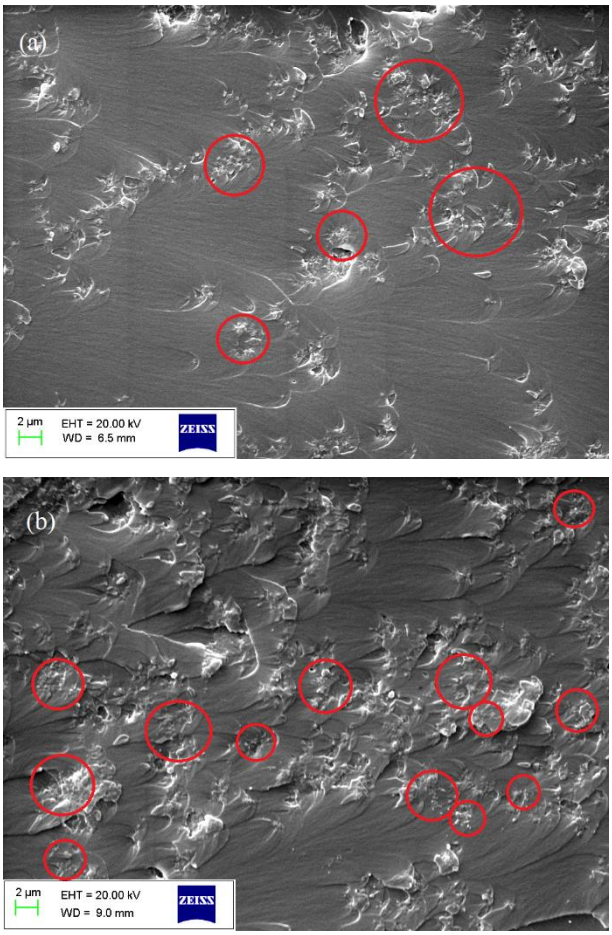

FIG. 2 SEM image of: (a) EPS3; (b) EPS5, ×5000.

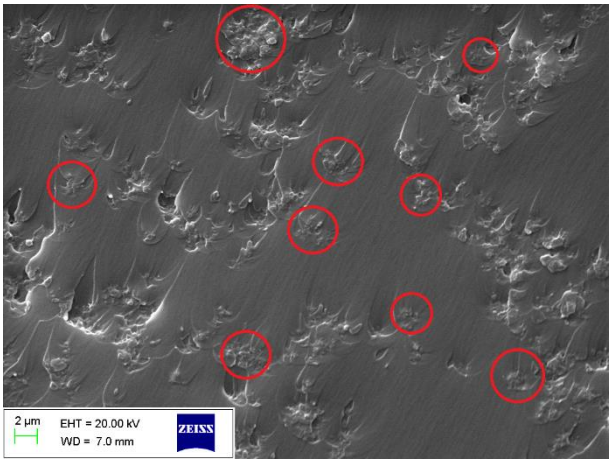

FIG. 3 SEM image of EPST5, ×5000.

Fig. 4 shows an example of histograms (EPS3) of the measured inter-particle/aggregate 1st nearest neighbour distance which is often used to evaluate the dispersion state of nanoparticles [14]. The quantitative data of EPS and EPST are then calculated and summarised in Table 2. It is obvious inter-particle distances of both silica-based epoxy nanocomposites samples decrease as the filler loading is increased, and also, EPST shows relatively better dispersion than EPS samples.

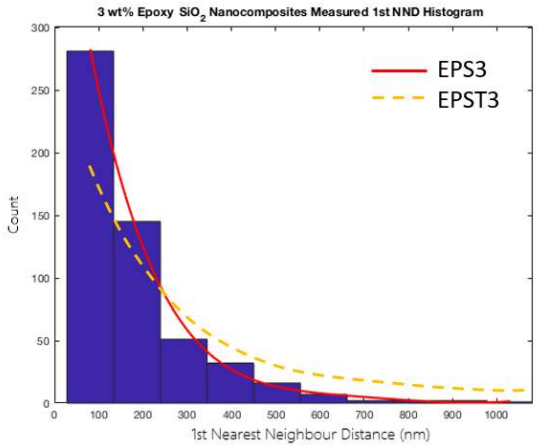

FIG. 4 Histogram of measured 1st Nearest Neighbor Distance of EPS3 (occurrence probability curve of EPST3 shown as a dashed line).

Table 2 Quantification data of SEM images, EPS and EPST samples in 1, 3, 5 wt%

Sample Code	Weighted 1st Nearest Neighbour Distance (nm)	Sample Code	Weighted 1st Nearest Neighbour Distance (nm)
EPS1	291.11	EPST1	353.12
EPS3	218.48	EPST3	277.10
EPS5	177.60	EPST5	245.16

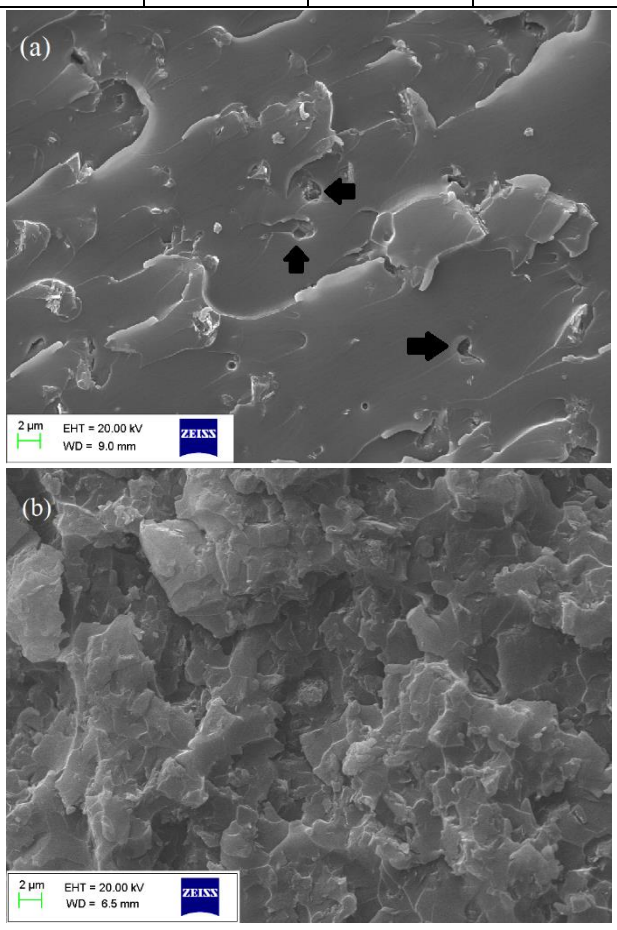

FIG. 5 SEM image of: (a) EPB1; (b) EPB5, ×5000.

The SEM images of EPB samples are shown in Fig. 5. For this type of nanoparticles it can be concluded that there are two main distinct forms, which have also been observed in clay platelet-based nanocomposites [26]: First, due to the sonication process, particles can be exfoliated and solely dispersed in the matrix. Second, some exfoliated particle plates could intercalate with the chains or their segments [26].

The presence of these kinds of hBN particles/aggregates could lead to some stress concentration sites and initiation of cracks [27] as shown in Fig. 5(a). The cracking and disruption of the matrix become more severe in samples of higher filler loading. It is noted that hBN particles have a much more noticeable impact on the morphology of base material than SiO_2 nanoparticle and tend to produce a layered structure in the matrix shown in Fig. 5(b). In our previous work, these types of structures are proved to result in more short polymer chains in bulk [24] than that of silica-based samples.

3.2 DC Conductivity

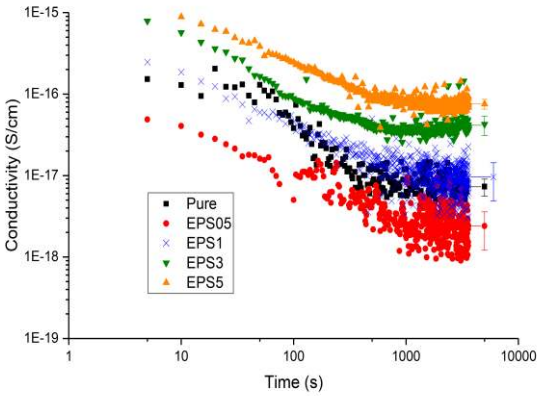

FIG. 6 DC conductivity of pure and EPS samples in each filler loading ratio, dry, 293K.

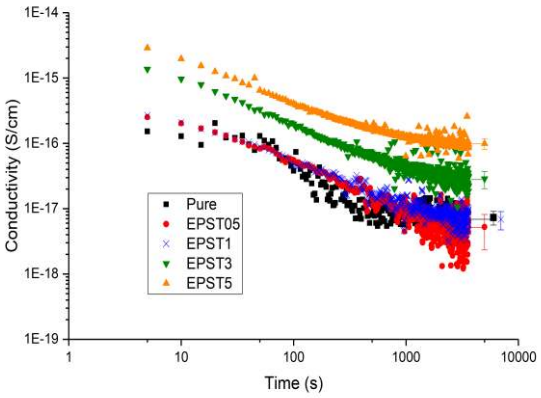

FIG. 7 DC conductivity of pure and EPST samples in each filler loading ratio, dry, 293K.

The DC conductivity of pure, EPS, EPST and EPB samples in each filler loading ratio at 293K are plotted in Fig. 6-8 as a function of time. All the data in the last 600s of each curve are plotted, with an error bar also included. It is noted that, in all kinds of nanocomposites, conductivity increases with the growth of filler loading ratios. However, it should be noted that the variation of EPB samples is obviously smaller than that of SiO_2 based samples.

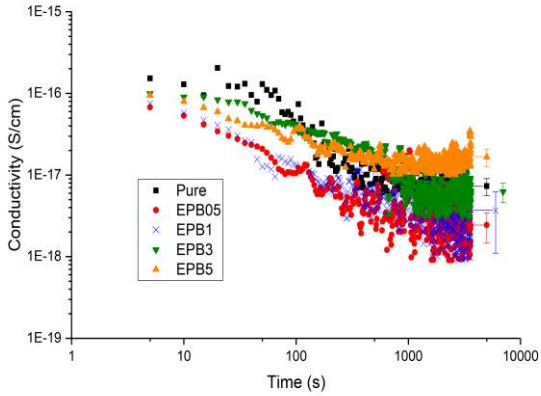

FIG. 8 DC conductivity of pure and EPB samples in each filler loading ratio, dry, 293K.

The DC conductivity of pure, EPS, EPST and EPB samples of 1 and 3 wt% are shown in Fig. 9 and 10. It is noted that EPST1 samples have similar and slightly higher conductivity when compared to EPS1 samples, which becomes more obvious at 3 wt%. This is likely to be caused by impurities introduced by surface treatment, which acts as additional charge carriers, resulting in high conductivity. The samples with higher loading ratios clearly contain larger amounts of this kind of carrier; our experiment is consistent with analysis, which is also reported in [28]. However, water absorption should cause an increase of conductivity after 1000s in EPS1 and EPS3 samples during the test, that is the reason why the conductivity of EPS in the last 600s is higher than that of EPST in both 1 and 3 wt%.

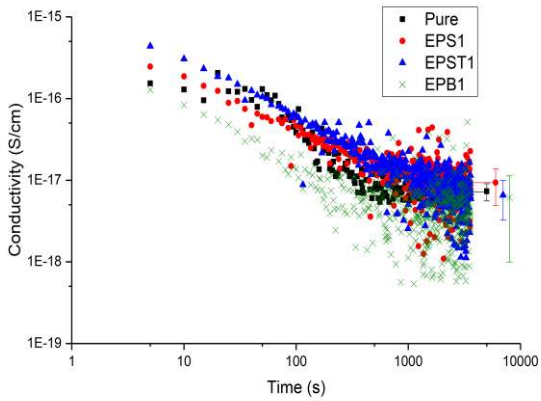

FIG. 9 DC conductivity of epoxy and its nanocomposites (1 wt%), dry, 293K.

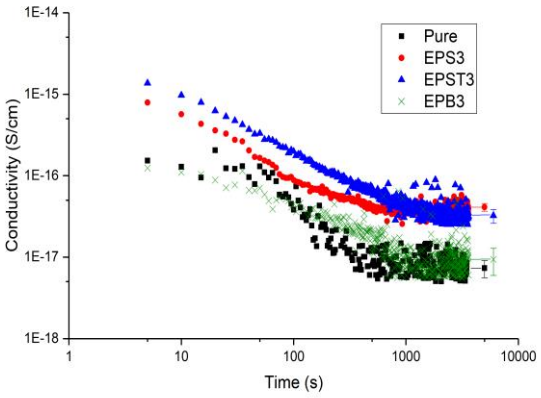

FIG. 10 DC conductivity of epoxy and its nanocomposites (3 wt%), dry, 293K.

The effect of moisture on pure epoxy samples is shown in Fig. 11. The conductivity rises with the increase in RH conditions due to the enhancement of the mobility of charge carriers. The ratios of conductivity in A. RH, 60RH and saturated samples appear similar to that of the water uptake percentage measured in our previous work [24] as they are 0.40%, 0.52% and 1.86% respectively. Same phenomena are also observed in all epoxy nanocomposites under same filler loadings as shown in Fig. 12 and 13. Moreover, it is obvious that DC conductivity of silica-based samples under same RH conditions both show and increase with the growth of filler loadings (with samples in 60RH in Fig. 14 as an example). However, EPB samples in all RH conditions exhibit opposite trends when compared to EPS and EPST samples, showing lower conductivity in 3 wt% even though conductivity still increases under RH conditions. This behaviour could be due to the fact that the morphology discussed in section 3.1 from the presence of nano-hBN particles is more dominant than moisture on the conductivity of EPB samples.

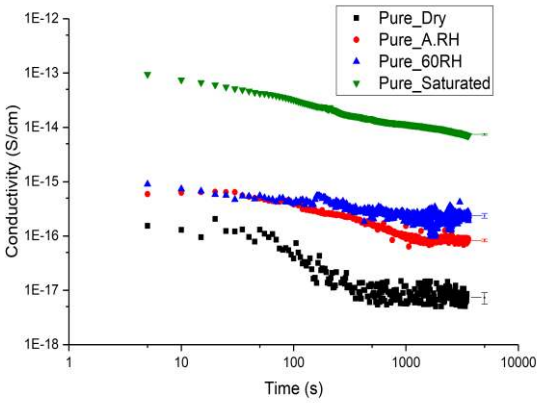

FIG. 11 DC conductivity of pure epoxy resins in each RH condition, 293K.

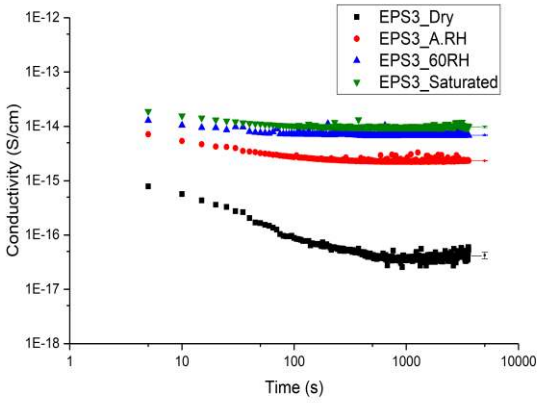

FIG. 12 DC conductivity of pure and EPS3 in each RH condition, 293K.

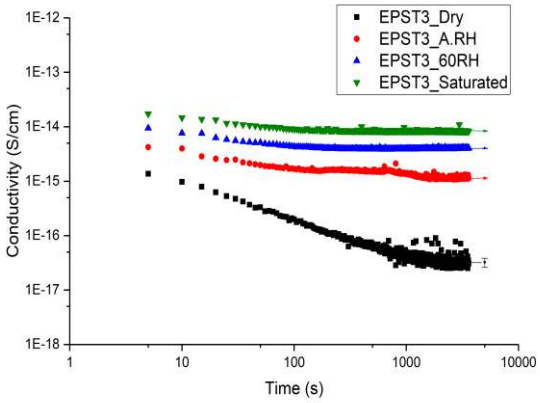

FIG. 13 DC conductivity of pure and EPST3 in each RH condition, 293K.

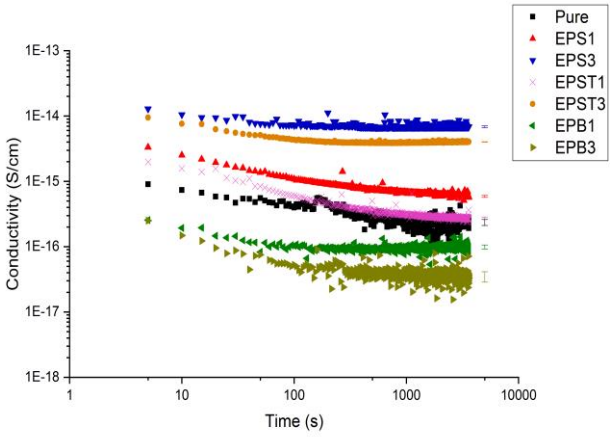

FIG. 14 DC conductivity of epoxy and its nanocomposites in 1 and 3 wt%, 60RH, 293K.

3.3 Space Charge

Results of the "volts-on" space charge measurement on pure specimens are shown in Fig. 15.

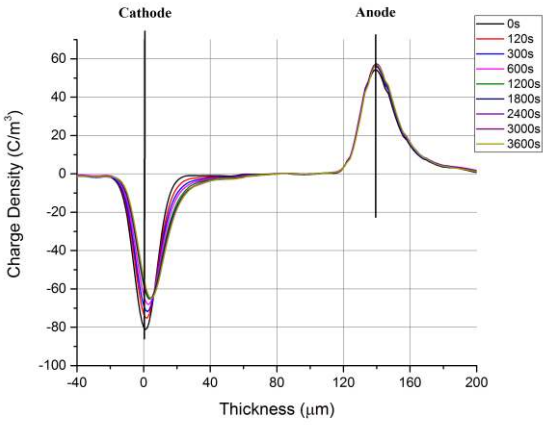

FIG. 15 Space charge profile of pure samples at 40 kV·mm^{-1}, dry.

As the PEA system only measures the net charges, this might be covered by the charge injection. Thus, in an attempt to reflect more details of the charge distribution in bulk, a subtraction method was employed to remove the capacitive charges from the electrodes [29]. In this method, the reference data is multiplied by the ratio between the applied voltage and a reference voltage; this can be considered as the charge density data at the applied voltage without the effect of space charges in bulk. The actual measured charge density data obtained from the volts-on measurement minus the multiplied, will reveal the injected charges in the sample and its induced charge at the electrodes. This can be expressed as below [29]:

$$\rho_{acc}(x) = \rho_{app}(x) - \frac{V_{app}}{V_{ref}} \cdot \rho_{ref}(x) \qquad (1)$$

where V_{ref} and V_{app} are the reference and applied voltages, $\rho_{acc}(x)$ is the space charge density after subtraction, and $\rho_{acc}(x)$ and $\rho_{ref}(x)$ represent the charge density at the applied voltage and reference voltage respectively. This method is applied to the results of unfilled epoxy (shown in Fig. 16) and all the nanocomposites.

Moreover, the total charge amount and charge density within the bulk of the sample can be calculated using Equations 2 and 3, as follows:

$$Q = \int_0^d \left(|n_p(x)| + |n_n(x)|\right) \cdot A dx \qquad (2)$$

$$n = Q/(A \cdot d \cdot q) \qquad (3)$$

where $n_p(x)$ and $n_n(x)$ are the charge density of positive and negative charges respectively, A is the electrode area equal to 50.265 mm^2 (with a radius of 4 mm), d is the thickness of samples (145 ± 10 μm), Q is the total charge amount, $q = 1.602 \times 10^{-19} C$ and n is total charge density in bulk.

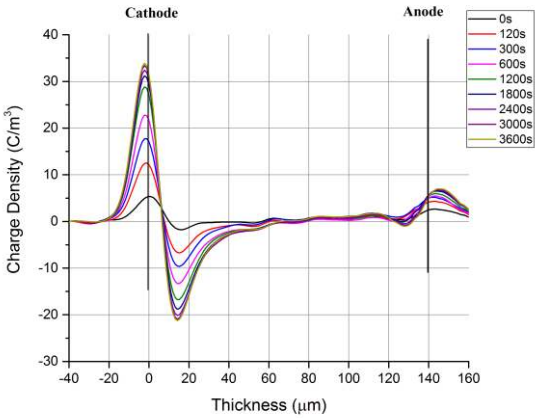

FIG. 16 Space charge profile of pure samples at 40 kV·mm^{-1}, dry.

In Fig. 16, it is obvious that some homocharges present adjacent to the cathode in pure epoxy and that the amount of homocharges increases with time. Charges are dictated by homocharges, and the presence can be attributed to charge injection from both electrodes in the form of electrons and holes [19]. Heterocharges may occur due to the charge separation process in the specimen but play only a minimal role.

When compared to pure samples, the subtracted space charge profile in the EPS samples are shown in Fig. 17, while the charge density in bulk is plotted in Fig. 20(a). There is an obvious negative charge injection in the EPS1 samples; moreover, EPS3 and EPS5 samples exhibit anomalous charge distribution behaviour, as there are a large number of heterocharges distributed near both electrodes.

In the EPS5 sample, as shown in Fig. 17(c), a large amount of charge injection can be observed. First, near the anode, the homocharges moving towards the cathode indicate the injection of positive charges, although the magnitude first increases and then decreases (this may be caused by the neutralisation with negative charges); second, adjacent to the cathode, the magnitude of heterocharges increases with time, and the peaks move towards the anode, which may be the result of the continuous injection of negative charges; third, in *Rectangle A*, the peaks decrease as they move towards the cathode and then increase as they move towards the anode, which may indicate that the charge built up in this region is first dominated by positive charges and then by negative charges. Based on this analysis, the heterocharges appearing adjacent to both electrodes should be the injected charges from the opposite side of the samples and neutralise the homocharges located at the space they occupied, which does not happen in EPS1. A similar observation was also made in [1].

Moreover, since the PEA technique can only show the net charge distribution in bulk, the total charge amount of EPS3 before 750s is lower than that of and EPS1 (as shown in Fig. 20(a)), which is due to the neutralisation at both electrodes. The analysis above suggests that samples filled with more untreated SiO_2 particles will have a larger charge injection and higher charge mobility in bulk. In other words, as conductivity is the product of charge carrier concentration n and mobility μ, they will have higher conductivity. This is consistent with the results observed in section 3.2.

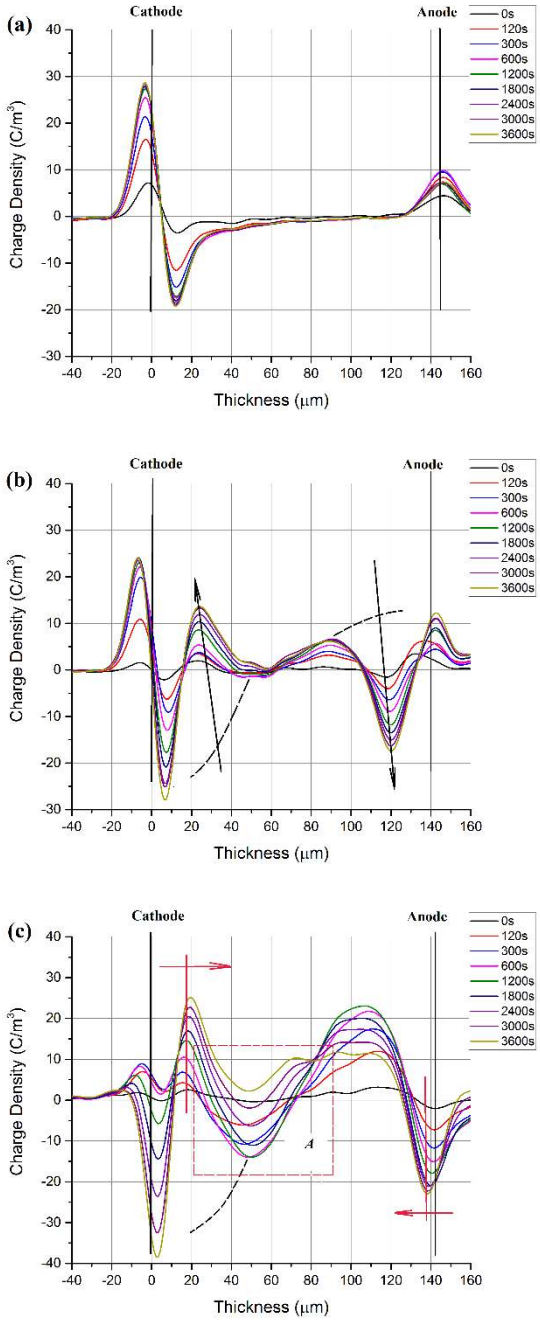

FIG. 17 Subtracted space charge profile of EPS at 40 kV·mm^{-1}: (a) 1 wt%; (b) 3 wt%; (c) 5 wt%, dry (dash curves indicate the ideal charge distributions without neutralisation).

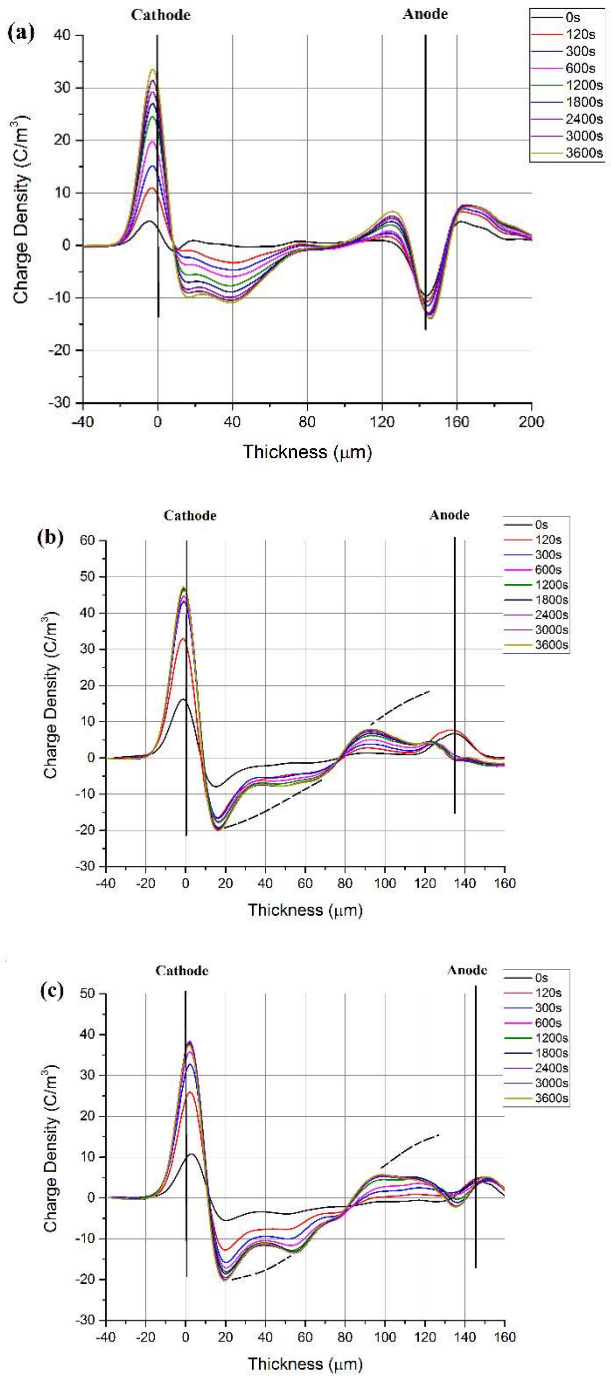

FIG. 18 Subtracted space charge profile of EPST at 40 kV·mm^{-1}: (a) 1 wt%; (b) 3 wt%; (c) 5 wt%, dry (dash curves indicate the ideal charge distributions without neutralisation).

The subtracted space charge distribution in the EPST samples are shown in Fig. 18, while the charge density in bulk is plotted in Fig. 20(b). In EPST1, homocharges are presented at both electrodes and move towards the middle of the sample.

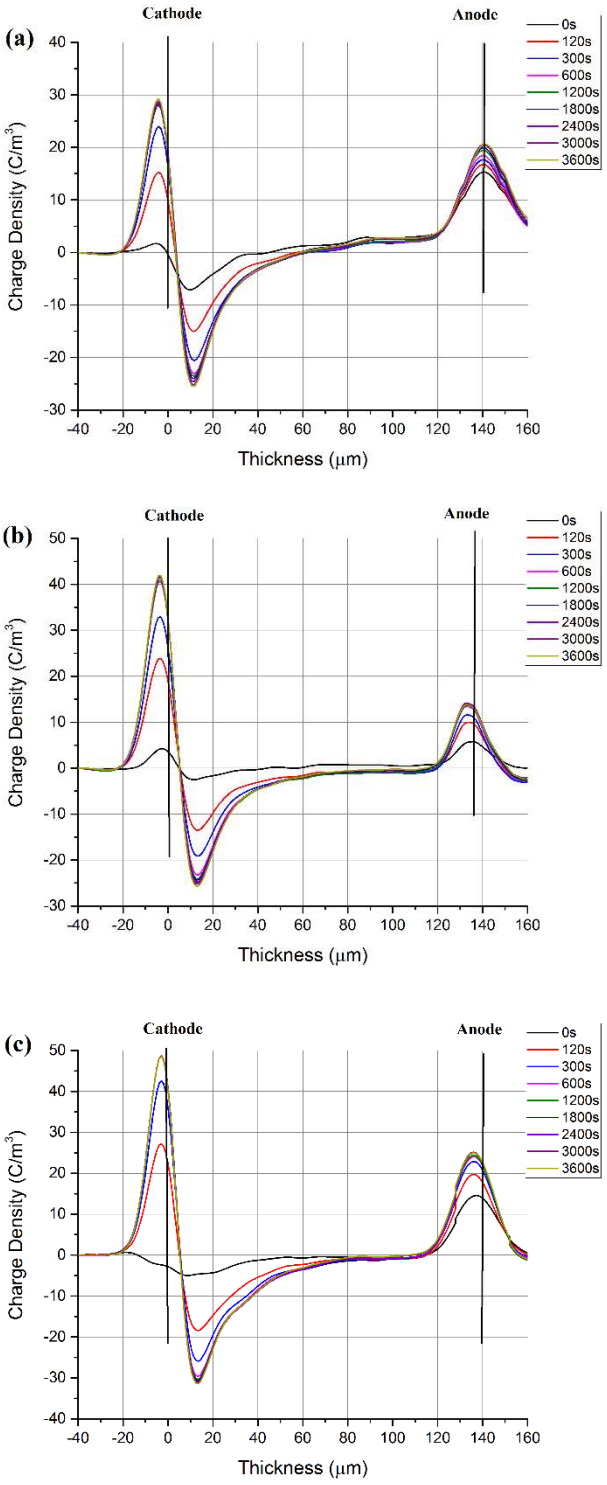

FIG. 19 Subtracted space charge profile of EPB at 40 kV·mm^{-1}: (a) 1 wt%; (b) 3 wt%; (c) 5 wt%, dry.

Moreover, as shown in Fig. 20(b), the lower charge injection rate of EPST1 at the beginning may be evidence for deep traps introduced by the surface treatment presence of which is proved by our previous work [24] and would restrict the charge mobility in bulk. Moreover, with the increase of filler loadings, fast initial charge built-up and similar charge neutralisation phenomena as in EPS3 and EPS5 are observed in EPST5. However, the injected charges traveling through the whole bulk are not as numerous as those in the EPS3 and EPS5 samples, which consequently show heterocharges at both electrodes.

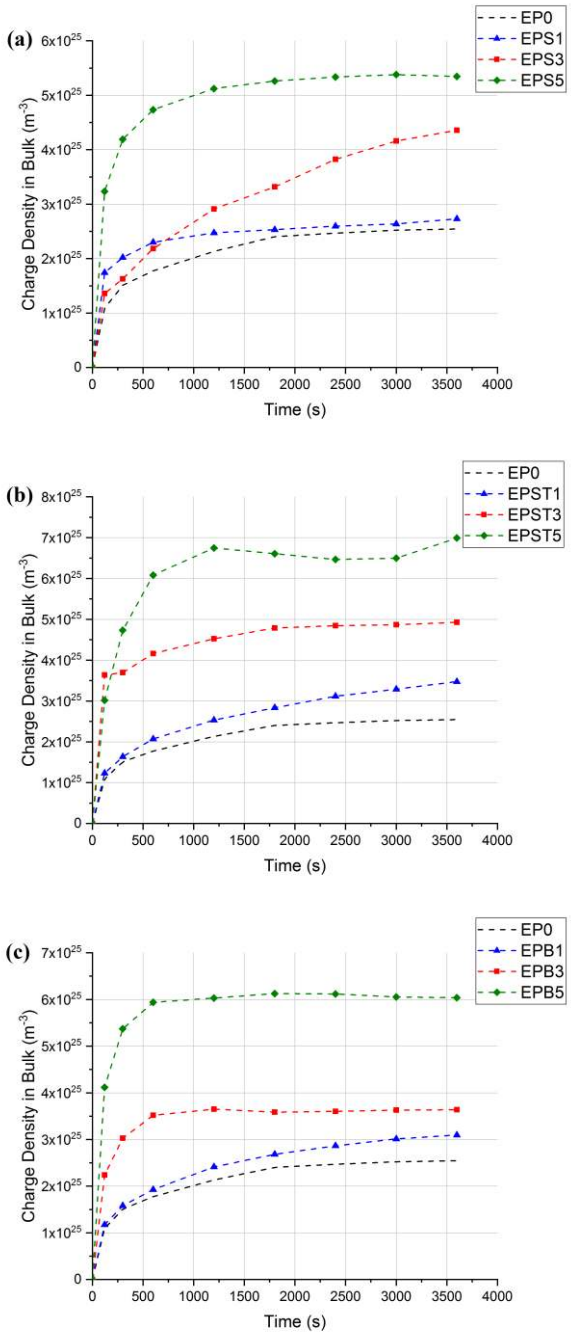

FIG. 20 Charge density in bulk of pure, EPS, EPST and EPB of 1, 3 and 5 wt%, dry.

Fig. 19 shows the subtracted space charge profile in EPB samples. Obviously, in EPB samples, charges are dominated by homocharges. It can be seen that the injected negative charges gradually increase and move towards the middle of

the bulk with the growth of filler loading ratios. Moreover, EPB samples clearly show suppressed injection when compared to silica-based ones and an increase in initial built-up charge with the growth of filler loadings, which may refer to the presence of shallow traps in bulk [13] due to the morphology in bulk.

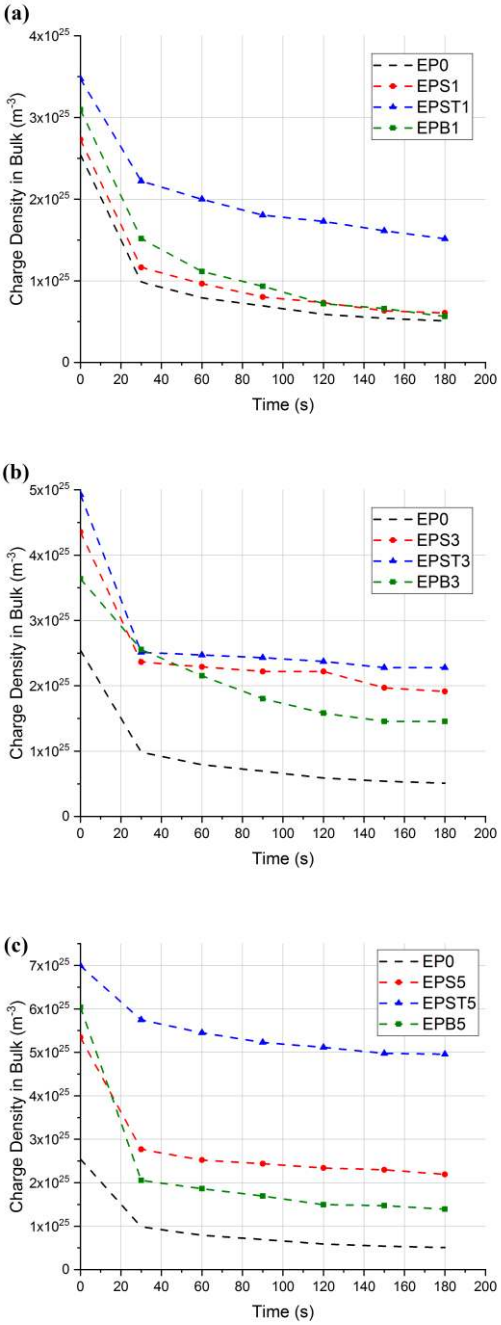

FIG. 21 Comparison of space charge decay of charge density in bulk of epoxy and its nanocomposites of 1, 3 and 5 wt%, dry.

The space decay measurements of pure, EPS, EPST and EPB samples are then carried out, and the charge densities in bulk are then summarised in Fig. 21 while space charge decay rates are calculated and shown in Table 3. Among all types of samples, the residual charges increase as the filler loading ratio increases and could indicate more traps in samples due to the addition of more fillers. EPS samples show a gradually rising decay rate as loadings increase, which provides evidence for the existence of traps due to the presence of nanofillers. However, EPST samples show a contrary trend: the decay rate decreases, while the residual charge amount in bulk is the highest among all samples types for each filler loading. This is caused by the additional deep traps in the EPST samples, since charges decay slower from deep traps, which are usually related to chemical changes in bulk, than from shallow traps, which are caused by the physical defects [30]. The high rate in EPST3 should be caused by increased charge mobility due to the growth of filler loadings, and with the further increase in filled particles, the mobility of charge carriers is restricted. Thus, it can be concluded that the presence of nano-SiO_2 fillers could mainly lead to physical changes and resultant shallow traps in bulk, while surface treatments act as chemical changes that will introduce more deep traps. Regarding the EPB samples, residual charge amounts in bulk are the lowest compared to EPS and EPST (shown in Fig. 21), and the space charge decay rates increase with the growth of filler loadings, especially in EPB5 (shown in Table 3). Thus, according to the previous analysis, the traps in EPB samples are likely to be shallow traps. As mentioned in the above discussion of the morphology of EPB samples (see section 3.1), these traps are due to the presence of hBN particles which result in physical defects [30] such as layered structures/cracks.

Table 3 Space charge decay rate $(m^{-3}s^{-1})$ of epoxy and its nanocomposites.

Sample Code	Filler Loading Ratio			
	0 wt%	1 wt%	3 wt%	5 wt%
EP	1.13E+23	-	-	-
EPS	-	1.18E+23	1.36E+23	1.75E+23
EPST	-	1.13E+23	1.47E+23	1.09E+23
EPB	-	1.41E+23	1.21E+23	2.58E+23

Regarding the moisture effects on space charge behaviour, the "volts-on" PEA measurement results of epoxy and its nanocomposites under ambient and 60% relative humidity conditions are shown in Fig. 22 to 25. In Fig. 22, pure samples show that the homocharge injection and initial charge build-up rate significantly increases with moisture. However, the magnitude near the cathode decreases and shows an increase at the anode with the growth of the RH condition. It is noted that more charges are injected into bulk, and that the presence of moisture results in the injected charge amounts and mobilities. Moreover, negative charges present in the middle of samples under both RH conditions and seem to contain more in bulk of samples under 60RH.

This should first be attributed to the water molecules that produce ions (OH^-, H_3O^+) and holes coming from the anode [14, 31]. More water content means that more ionised charges

will be present in the bulk of samples. Second, as electrons can travel through inter-chain spaces [32, 33] where water could locate, negative charges obviously appear in the bulk of RH conditioned samples and even neutralise some positive charges at the anode from 600s onwards (see Fig. 22 (b)). Moreover, there is also a presence of neutralisation near the cathode at later times, indicating the movement of positive charges.

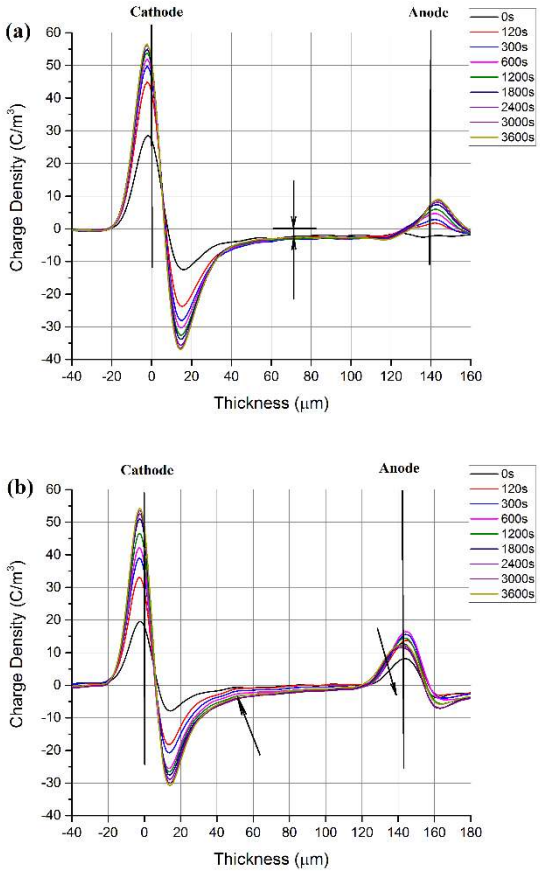

FIG. 22 Subtracted space charge profile of pure samples at 40 kV·mm^{-1}: (a) A.RH; (b) 60RH.

As shown in Fig. 23, for EPS1 and EPS3, the initial injection rate and neutralisation phenomena become quicker and more obvious with the growth of RH conditions and filler loadings, indicating the higher mobility of both positive and negative charges. Moreover, more obvious increases in the magnitude of heterocharges near the anode than those adjacent to the cathode indicate the dominance of negative charges in the 60RH condition due to the presence of water in the matrix, which is also found in pure samples and leads to higher mobility.

In the case of EPST samples, as shown in Fig. 24 (a), the charge distribution of EPST1 is dominated by homocharges, which may be caused by more deep traps in bulk due to the surface treatment. Once more nanofillers are added, EPST shows obvious charge injection (see Fig. 24(b)). Unlike the presence of neutralisation in EPS samples, EPST3 under A.RH conditions is more dominant by positive charges. As surface treatment introduces additional deep traps, positive charges can travel along these traps while becoming more mobile as water uptake increases. However, when RH conditions rise to 60%, negative charges still show dominance and positive charges move inside the bulk of material as shown in Fig. 24(c).

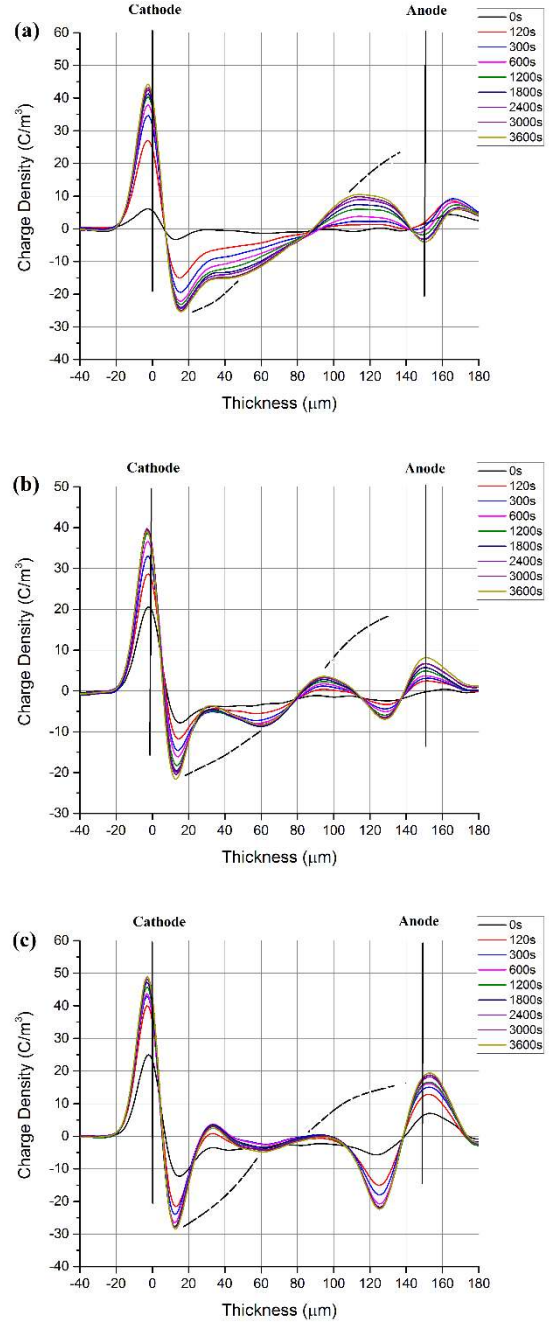

FIG. 23 Subtracted space charge profile of EPS at 40 kV·mm^{-1}: (a) 1 wt%, A.RH; (b) 3 wt%, A.RH; (c) 3 wt%, 60RH.

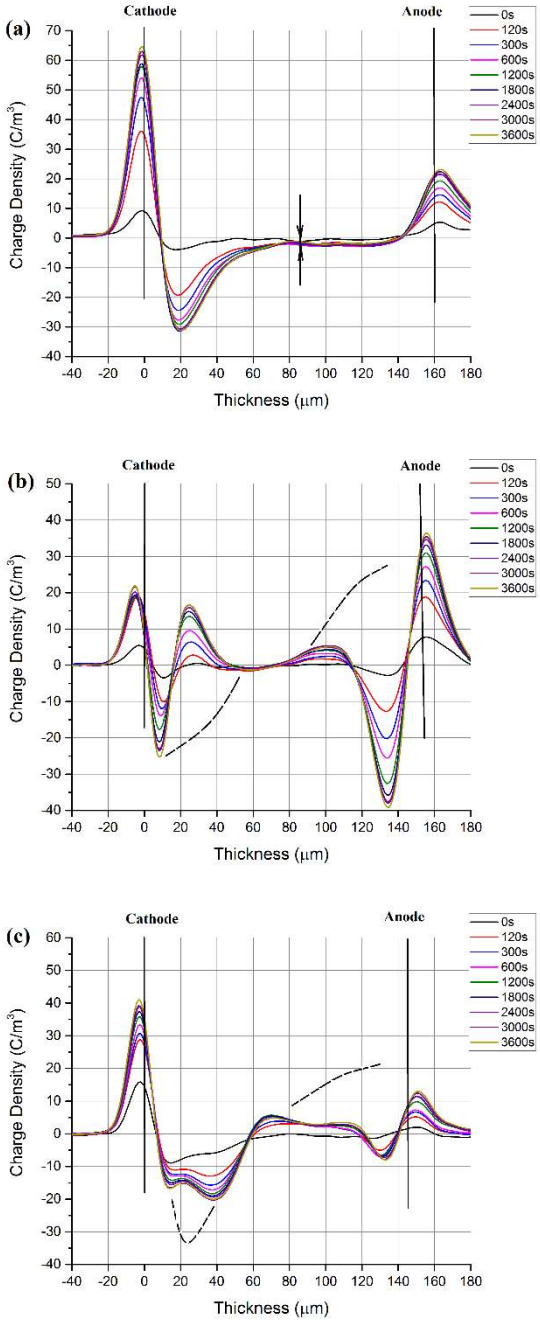

FIG. 24 Subtracted space charge profile of EPST at 40 kV·mm^{-1}: (a) 1 wt%, A.RH; (b) 3 wt%, A.RH; (c) 3 wt%, 60RH.

As can be seen in Fig. 25(a) and (b), EPB samples only show homocharge in bulk, and there is an increase of magnitude near the cathode as water content rises. Moreover, there are negative charges in the middle of samples under the 60RH condition. One possible source could be the ions from water (H_3O^+ and OH^-), while another more important source is the increased injection in the form of negative charges. Moreover, when comparing Fig. 25(b) and (c), the neutralisation in samples with higher filler loadings indicate the increase in mobility of positive charges, a phenomenon also found in EPS and EPST samples. This is likely to be due to the presence of water which contributes to the movement of positive charges [33].

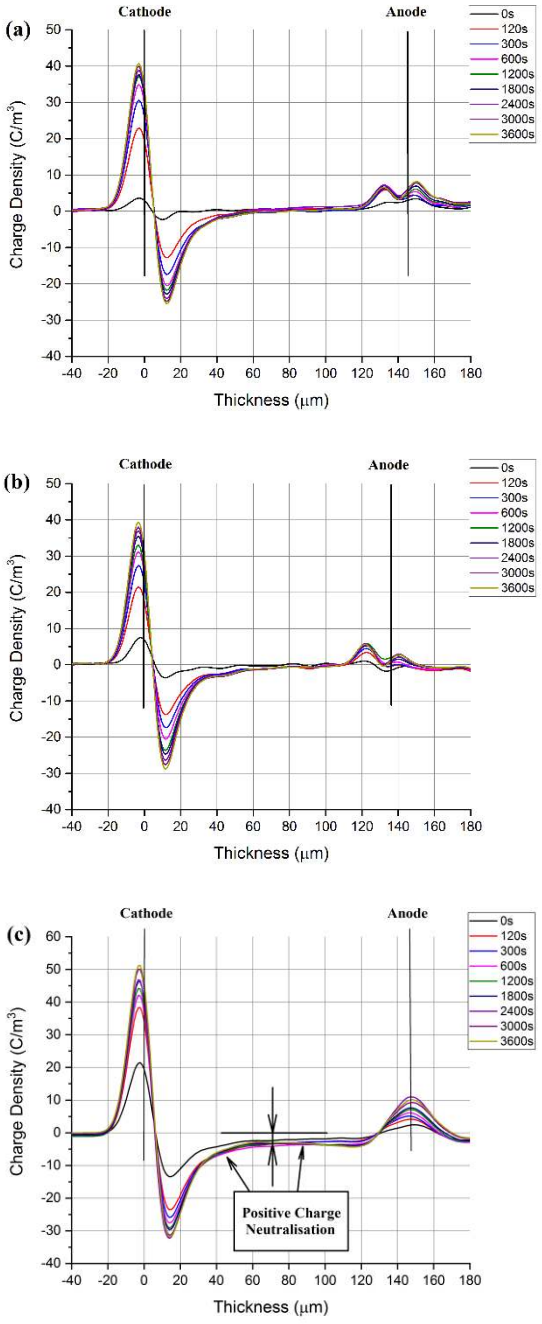

FIG. 25 Subtracted space charge profile of EPB at 40 kV·mm^{-1}: (a) 1 wt%, A.RH; (b) 3 wt%, A.RH; (c) 3 wt%, 60RH.

4. Discussion

The term “trap sites” is usually used to explain the charge dynamics of polymer dielectrics. Regarding conduction in polymer insulators, taking PE as an example, it is believed to be dominated by electrons and the transport of carriers takes

place along the amorphous regions and is limited by traps [34, 35]. One of the mechanisms for charge transport is known as *thermally activated hopping* from one trap to another, where the electron/hole gained sufficient energy could overcome the potential barrier by thermal fluctuations to reach. Another mechanism is that an electron/hole can move from one trap to a close adjacent one by means of *quantum mechanical tunnelling,* as an electron is not only well-defined as a particle and the electron-wave can tunnel through narrow barriers by simply 'appearing' to a nearby trap [36]. Charge mobility is strongly influenced by the concentration of traps sites and the presence of nanoparticles could introduce traps around [37]. In case of the hopping process, the relationship between mobility μ and concentrations of traps can be expressed by following equation [38]:

$$\mu \propto \exp\left(-\frac{2}{\alpha N_0^{1/3}}\right) \tag{4}$$

where N_0 is the concentration of traps and α is the localisation length of localised states. It is obvious, in the case of the hopping process, the mobility of charges is inversely proportional to the inter-trap distance.

Moreover, in some previous research, tunnelling process is also suggested to explain charge transport in polymer nanocomposites with higher filler ratios [13, 39]. There provides a good way to understand the suppressed charge transport in samples of low filler loading ratios and increased charge dynamics in that of high ratios. Equation 5 represents the characteristic of charge transport by tunnelling mechanism [39].

$$J = \frac{CE^2}{E_t}\exp\left(-\frac{BE_t}{E}\right)\exp\left(-\frac{2d}{d_0}\right) \tag{5}$$

where C and B are constants, E is the applied electric field, E_t is the trap depth or barrier height, d is the separation distance between two adjacent traps in the field direction and d_0 is the characteristic tunnelling distance. Based on this equation, the charge transport by tunnelling mechanism can be influenced by three parameters: separation distance between two adjacent traps, traps depth and the electric field.

Thus, it is easy to understand the charge dynamics in nanocomposites of 0.5 wt%. For example in Fig. 6, EPS05 shows slightly lower conductivity than pure samples; this is likely due to the presence of nanoparticles [40], and resultant traps near the surface could capture the charge carriers (see Fig. 26(a)). As the inter-traps distance in samples of low filler ratios is large which is hard for carriers to transport from one to another, neither by hopping process nor tunelling mechanism, these trapped charges near the surface generate an opposite electric field and reduce the applied electric field, which will hinder the charge injection, thus reducing the mobility of charge carriers and finally resulting in a reduction in conductivity [41].

However, with an increase in filler loadings, more nanofillers will lead to a higher density of traps; this means the average distance between arbitrary traps should be lower in samples with higher filler loadings and that charge carriers will require less energy when moving from one to another (as shown in Fig. 26 (b)). The resultant increased carrier mobility will lead to higher conductivity. Moreover, the observed phenomena of neutralisation in space charge behaviour of EPS is recombination of positive and negative charges. If regarding nanofillers as recombination centres [33], the shorter average surface distance between nanoparticles in samples of high filler loadings (shown in Table 4) should also result in a higher conductivity value. EPST samples should share a similar mechanism and it is easy to understand their lower charge mobility in bulk.

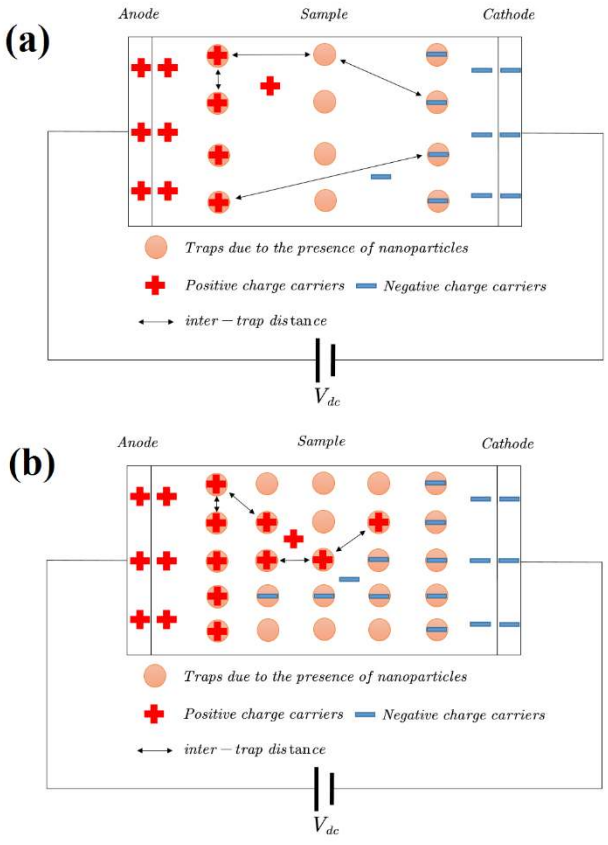

FIG. 26 Schematic of charge distribution in nanocomposites of uniformly distributed traps with: (a) low loading ratio; (b) high loading ratio.

EPB samples are slightly different from silica-based samples. This is likely due to the vastly more complex morphology in bulk (as has been shown in section 3.1) and the enormous traps adjacent to the surface, which not only come from the presence of nanoparticles but also the resultant morphology of matrix (shown in Fig. 5), significantly reduce the applied electric field and thus the amount of injected

charges. Presence of plate-like nano-hBN fillers seem to act as barriers for charge injection and movement, and lead to lower conductivity (as shown in Fig. 8) which is determined by the product of $n \times \mu$, even in the samples of high filler loading ratios.

Table 4 Weighted surface distance of EPS and EPST in filler loading ratios of 1, 3 and 5 wt%

Sample Code	Weighted Average Surface Distance (nm)	Sample Code	Weighted Average Surface Distance (nm)
EPS1	180.43	EPST1	257.35
EPS3	155.27	EPST3	200.08
EPS5	121.59	EPST5	157.97

Table 5 Weighted surface distance of EPS and EPST samples in 1 and 3wt% under dry, 60RH and saturated conditions

Sample Code	Dry (nm)	60RH (nm)	Saturated (nm)
EPS1	180.43	157.93	137.09
EPS3	155.27	134.92	115.50
EPST1	257.35	239.58	224.29
EPST3	200.08	178.22	155.31

In term of moisture effect, presence of water in bulk will surely increase the charge injection and mobility according to the results of pure samples. In EPS and EPST samples, increased conductivity is evident in samples of higher filler loadings. Firstly, this is due to the presence of more water, leading to higher mobility values of charge carriers in both base materials and within traps/particles. Secondly, to consider the effect of the shorter distance between traps due to presence of particles, the surface distances of EPS and EPST samples under dry, 60RH and saturated conditions based on the water-shell model and shell thickness analysis in our previous work (higher the RH condition, thicker the water shell) [24] are presented in Table 5. It is obvious that shorter average surface distance is evident in samples with higher water content and filler loadings; this will make it easier for carriers to move from one trap site to another if particles are regarded as recombination centres [33]. In some cases, the overlapped water shells could even provide channels for charge carriers to travel through. This is schematically shown in Fig. 27. Moreover, the effect of hopping and quantum tunnelling processes may be more obvious in higher RH conditions. As hopping distance may be larger than the distance stated in Table 5, it is assumed that the tunnelling effect may become much more significant due to the presence of moisture. Some researchers have reported various tunnelling distances between traps, and one has quantified it as ~10 nm [42]. If this value is taken as the threshold of tunnelling, the percentages of the surface distances between one particle and the closest one that are smaller than 10 nm under dry, 60RH and saturated conditions are listed in Table 6.

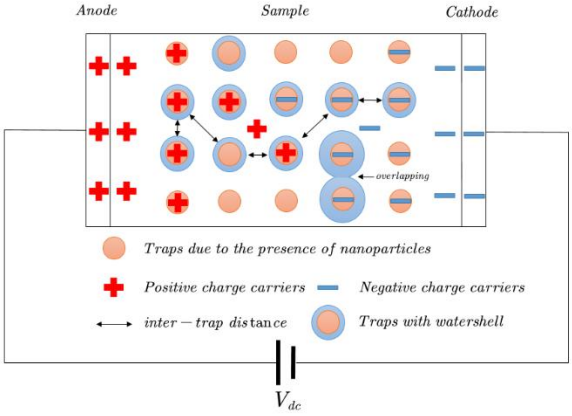

FIG. 27 Schematic of charge distribution in nanocomposites of uniformly distributed traps with water shells.

Table 6 Percentage of weighted surface distance <10 nm of EPS and EPST samples in 1 and 3wt% under dry, 60RH and saturated conditions

Sample Code	Dry (%)	60RH (%)	Saturated (%)
EPS1	17.25	48.61	65.57
EPS3	18.50	49.73	70.32
EPST1	14.57	40.13	51.79
EPST3	16.54	48.48	62.88

As shown in Table 6, it is noted that, under the dry condition, the percentages of both EPS and EPST are lower than 20% and increase slightly with the growth of filler loadings. Moreover, the slightly smaller ones in the EPST samples are likely due to the surface treatment. With the presence of moisture, the percentages show significant increases of ~30% in samples under 60RH condition and a further increase ~10-15% in saturated ones. A similar ratio is also found in the experimental results of the conductivity of 3 wt% samples, as is shown in Fig. 12 and 13, rather than the ratio of water uptake between these two RH conditions (in previous work [24]). Results for 1 wt% show similar trends. This is also supported by the results of space charge behaviour in Fig. 23 and 24. The reduction in the distance of arbitrary deep traps (introduced by surface treament) related to the inter-particle distance may result in the higher probability of trapped charges passing through the potential well by the quantum tunnelling mechanism [13] (based on results of EPST3 relative to EPST1 in Table 6), which could contributes to the dominance of positive charges and move-in in EPST3 (see in Fig. 24(b)) while EPS3 is more dominant by negative

charges (see in Fig. 23(b)). Thus, the tunnelling effect should become more obvious in silica-based samples with moisture.

In most cases, BN particles and the resultant morphology seem to act as barriers or to play a role in hindering the injection and formation of channels for charge carriers in each RH condition, which are both observed in the results of DC conductivity and space charge measurements.

5. Conclusion

Combining all analysis on dry samples and samples with moisture gave us a clear view on the influence of adding nanoparticles to epoxy resins and the characteristics of the movement of positive and negative charges in bulk. Based on the analysis, the DC conductivity and space charge measurement were found to be consistent with each other. The presence of nanoparticles introduced additional traps in bulk, which hindered the charge injection and reduced the mobility of charge carriers in samples of low filler loading ratios, and thus contributed to the reduction of conductivity. However, with the increase of filler loadings, introducing more nanoparticles further caused a higher density of traps, meaning that the average distance between arbitrary traps/ inter-particle surface distances (either shallow or deep ones) should be lowered and that charge carriers require less energy when moving from one to another by hopping or the quantum tunnelling mechanism. The resultant higher mobility of carriers consequently led to the higher charge mobility within silica-based nanocomposites. Moreover, the surface treatment of SiO_2 particles introduced deep traps, which helped the separation of particles or related traps, and thus to some extent impaired the transport of charge carriers. In addition, hBN particles act as barriers to charge injection and movement due to the layered structures and the vast shallow traps in bulk.

The presence of water firstly produced more charge carriers as ions (OH^-, H_3O^+) due to polarisation and led to an increase in charge injection and mobility. Second, the presence of water resulted in the higher mobility of charge carriers in both base materials and within traps/particles. Moreover, water shells around spherical particles could contribute to a higher probability of the quantum tunnelling process and the formation of conductive percolation channels.

References

[1] Wang Q, Curtis P, and Chen G, 2010 in CEIDP Annual Report Conference 1-4.
[2] Fothergill J C, Nelson J K, and Fu M, 2004 in CEIDP Annual Report Conference 406-409.
[3] Lewis T, 2004 in ICSD **2** 792-795.
[4] Nelson J and Hu Y 2005 Journal of Physics: Applied Physics D **38** 213
[5] Okazaki M, Murota M, Kawaguchi Y, and Tsubokawa N 2001 Journal of applied polymer science **80** 573-579
[6] Shafee M F and Jaafar M 2013 Journal of Engineering Science **9** 89-98
[7] Guastavino F et al. 2005. Annual Report Conference 175-178.
[8] Montanari G C, Fabiani D, Palmieri F, Kaempfer D, Thomann R, and Mulhaupt R 2004 IEEE Transactions on Dielectrics and Electrical Insulation **11** 754-762
[9] Ieda M 1984 Electrical conduction and carrier traps in polymeric materials IEEE transactions on electrical insulation 162-178
[10] Kojima K, Takai Y, and Ieda M 1986 Journal of applied physics **59** 2655-2659
[11] Lewis T 1998 The micro-physics of charge in dielectrics Le Vide **53** 16-24
[12] Lewis T J 1986 Electrical effects at interfaces and surfaces IEEE transactions on electrical insulation 289-295
[13] Li G, Chen G, and Li S 2016 Applied Physics Letters **109** 062901
[14] Hui L, Schadler L S, and Nelson J K 2013 IEEE Transactions on Dielectrics and Electrical Insulation **20** 641-653
[15] Praeger M, Hosier I, Holt A, Vaughan A, and Swingler S 2017 IEEE Transactions on Dielectrics and Electrical Insulation **24** 2410-2420
[16] Praeger M, Hosier I, Vaughan A, and Swingler S 2015 in Electrical Insulation Conference (EIC) 201-204.
[17] Roy M, Nelson J K, MacCrone R, and Schadler L 2007 Journal of Materials Science **42** 3789-3799
[18] Kao K C 2004 Dielectric phenomena in solids (Academic press)
[19] Fabiani D, Montanari G, Dardano A, Guastavino G, Testa L, and Sangermano M 2008 in Electrical Insulation and Dielectric Phenomena,. CEIDP 710-713.
[20] Cheng C 2005 Journal of Anhui Institute of Architecture **4** 018
[21] Gao C 2001 Journal of Jiangsu University of Science and Technology **22** 63-70
[22] Zou C, Fothergill J C, and Rowe S W 2008 IEEE Transactions on Dielectrics and Electrical Insulation **15**
[23] Hosier I L, Praeger M, Vaughan A S, and Swingler S G 2017 IEEE Transactions on Nanotechnology **16** 169-179
[24] Qiang D, Wang Y, Chen G, and Andritsch T 2018 IET Nanodielectrics **1** 48-59
[25] Li Y, Yasuda M, and Takada T 1994 IEEE Transactions on Dielectrics and Electrical Insulation **1** 188-195
[26] Kumar A P, Depan D, Tomer N S, and Singh R P 2009 Progress in polymer science **34** 479-515
[27] Saha M et al. 2015 Composite Interfaces **22** 611-627
[28] Lau K Y, 2013 "Structure and electrical properties of silica-based polyethylene nanocomposites," University of Southampton.
[29] Liu N, Zhou C, Chen G, and Zhong L 2015 Applied physics letters **106** 192901
[30] Zhou T, Chen G, Liao R-j, and Xu Z 2011 Journal of Applied Physics **110** 043724
[31] Hui L, Nelson J, and Schadler L 2010 in Solid Dielectrics (ICSD) 10th IEEE International Conference 1-4.
[32] Lewis T 1976 in Electrical Insulation & Dielectric Phenomena-Annual Report 533-561.
[33] Lewis T 2002 IEEE Transactions on Dielectrics and Electrical Insulation **9** 717-729
[34] Garton C and Parkman N 1976 in Proceedings of the Institution of Electrical Engineers **123** 271-276.

[35] Pelissou S, St-Onge H, and Wertheimer M 1988 IEEE transactions on electrical insulation **23** 325-333
[36] Merzbacher E 1998 Quantum Mechanics Inc., New York
[37] Takada T, Hayase Y, Tanaka Y, and Okamoto T 2007 Annual Report-Conference on Electrical Insulation and Dielectric Phenomena 417-420.
[38] Baranovski S and Rubel O 2006 Description of charge transport in amorphous semiconductors Charge transport in disordered solids with applications in electronics 49-96
[39] Chen G, Li S, and Zhong L 2015 in Properties and Applications of Dielectric Materials (ICPADM) 36-39.
[40] Lau K, Vaughan A, Chen G, Hosier I, Holt A, and Ching K Y 2014 IEEE Transactions on Dielectrics and Electrical Insulation **21** 340-351
[41] Chen G, Tay T, Davies A, Tanaka Y, and Takada T 2001 IEEE Transactions on Dielectrics and Electrical Insulation **8** 867-873
[42] Lubyshev D I, González-Borrero P P, Marega E, Petitprez E, La Scala N, and Basmaji P 1996 Applied Physics Letters **68** 205-207